2013-03-27

Metamaterial films as narrowband terahertz emitters

Kearney, Brian; Alves, Fabio; Grbovic, Dragoslav; Karunasiri, Gamani

SPIE

Kearney, Brian, et al. "Metamaterial films as narrowband terahertz emitters." Terahertz, RF, Millimeter, and Submillimeter-Wave Technology and Applications VI. Vol. 8624. International Society for Optics and Photonics, 2013.
https://hdl.handle.net/10945/60320

PROCEEDINGS OF SPIE

SPIEDigitalLibrary.org/conference-proceedings-of-spie

Metamaterial films as narrowband terahertz emitters

Brian Kearney, Fabio Alves, Dragoslav Grbovic, Gamani Karunasiri

Brian Kearney, Fabio Alves, Dragoslav Grbovic, Gamani Karunasiri, "Metamaterial films as narrowband terahertz emitters," Proc. SPIE 8624, Terahertz, RF, Millimeter, and Submillimeter-Wave Technology and Applications VI, 862410 (27 March 2013); doi: 10.1117/12.2005011

SPIE.

Event: SPIE OPTO, 2013, San Francisco, California, United States

Metamaterial Films as Narrowband Terahertz Emitters

Brian Kearney*, Fabio Alves, Dragoslav Grbovic, and Gamani Karunasiri
Department of Physics, Naval Postgraduate School, Monterey, CA 93943, USA
*Corresponding author: btkearne@nps.edu

ABSTRACT

Continued progress in terahertz (THz) research has emphasized the need for both improved THz sources and detectors. One approach to generate a narrowband THz radiation is to use metamaterial absorbers as thermal emitters. We present metamaterial based THz emitters consisting of a 100 nm aluminum layer patterned into squares separated from a ground plane of aluminum by a thin layer of silicon oxide (<2 μm) fabricated using standard microfabrication techniques. These metamaterials were designed to emit in one, two, and three different bands of the 4-8 THz range and demonstrate clearly definable separate peaks with bandwidths of approximately 1 THz. Modifying the multiple band configurations can produce relatively broad emission peak if desired. Single band emitters designed for 4.1, 5.4, and 7.8 THz were observed to emit, respectively, 11, 18, and 36 W/m^2 at 400 °C in accordance with Kirchhoff's law of thermal radiation. Coating a 4-inch wafer with these materials and heating it to 400 °C would produce an estimated 86, 145, and 280 mW of power, respectively. Additionally, emitted power increased linearly with temperature, as expected from the Planck's radiation law in the THz spectral region at elevated temperatures. Emissivity of the metamaterial did not change significantly when heated, indicating that the constituent materials did not significantly change their optical or geometric properties.

1. INTRODUCTION

Terahertz (THz) imaging technology has progressed rapidly in recent years. Applications of THz imaging in the 1-10 THz range include medical[1] and security[2,3] screening due to the ability of THz to penetrate many materials without damaging them while imaging metals and water content very effectively[1-5]. Uncooled imaging systems generally require an external source due to the small amount of background thermal energy in this spectral region. The low photon energy of 1-10 THz radiation (4-40 meV) makes optical methods of detection and generation difficult, often involving complex device architectures and very low temperatures[6]. Unfortunately, the photon energy is also too high for electronic generation techniques suitable for microwaves. Several technologies exist[7], the most promising approaches to generating THz radiation include quantum cascade lasers (QCLs)[8-10] and free electron lasers (FELs)[11]. However, these approaches either require expensive infrastructure (FELs) or cryogenic temperatures in the case of QCLs. Room temperature technologies such as resonant tunneling diodes are not yet able to generate power levels beyond the microwatt range. While the thermal emission of THz at room temperature is quite low, a heated object could produce increasing amount. If a metamaterial layer is added to the surface of such an object, the emission can be tailored to a specific frequency of THz. In this paper, generation of narrowband (~1 THz) THz emission using metamaterial structures is described.

2. DESIGN AND FABRIACTION

2.1 Design and Modeling

The metamaterial geometry for this study consists of a continuous layer of Al separated from a periodic array of Al squares by a SiO_2 dielectric spacer. The Al layers are approximately 90 nm thick; this is larger than the skin depth of THz in aluminum (~80 nm at 4 THz using conductivity of 10^7 S/m). The dielectric spacer is 1.6 μm thick, less than one tenth the wavelength of 4-8 THz in SiO_2 (~19-38 μm). Structural parameters, especially square size and

Terahertz, RF, Millimeter, and Submillimeter-Wave Technology and Applications VI, edited by Laurence P. Sadwick, Créidhe M. O'Sullivan, Proc. of SPIE Vol. 8624, 862410 · © 2013 SPIE · CCC code: 0277-786X/13/$18
doi: 10.1117/12.2005011

dielectric spacer thickness, can be used to control the emission frequency and magnitude, respectively. To aid in the design of these emitters, 3D finite element modeling was performed using COMSOL multiphysics software. The periodic nature of the metamaterial layers allows for modeling to be performed on a single unit cell with periodic boundary conditions[12]. The metamaterial unit cell is shown in Fig. 1(a). Kirchhoff's law states that absorption properties must be the same as emission; therefore, determining absorptivity of the layers is sufficient[13]. The absorbed power can be determined through integration of the zero order reflected and transmitted power as higher order scattering effects are negligible due to the subwavelength features considered. Additionally, transmitted power is negligible due to the thickness of the Al ground plane, so in practice only reflected power is required. Integrating resistive losses in the metamaterial is also a useful method of determining the emission properties of the metamaterial layer. The Al conductivity was determined to be 1 X 10^7 S/m. The real part of index of refraction of SiO_2 was taken to be 2 from [15,16]. The extinction coefficient, in comparison, has stronger frequency dependence at THz frequencies and was estimated from [17] to vary from 0.025 at 4 THz to 0.08 at 8 THz.

2.2 Fabrication

Standard MEMS materials and microfabrication techniques were used to construct these metamaterial layers[14]. First, Al ground planes were deposited using e-beam evaporation. Following this, SiO_2 was deposited using plasma-enhanced chemical vapor deposition (PECVD). A second layer of Al was then deposited using e-beam evaporation. Finally, the top layer of Al was patterned and sputter etched with Ar plasma. Al thickness was determined using a stylus profilometer and a four-point probe determined conductivity. An optical interferometer was used to measure the thickness of the SiO_2 layer. Figure 1(b) shows an optical micrograph of the final structures. Samples with various configurations were fabricated including five samples with square sizes of 17 μm, 15 μm, 13μm, 11 μm, and 9 μm (Samples A-E, respectively). All of these configurations have a periodicity of 21 μm.

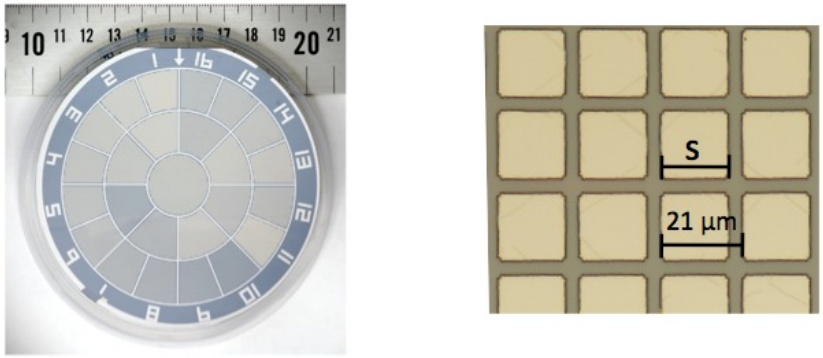

Figure 1. One of the fabricated metamaterial wafers (a) containing different metamaterial configurations arranged radially and a micrograph (b) of a fabricated structure. Reprinted from [18]

3. EXPERIMENTAL RESULTS

3.1 Absorption measurements

Prior to measuring the emission properties of the metamaterial layers, the absorption characteristics were determined using a Nexus 8700 Fourier transform infrared spectrometer (FTIR)[12]. As transmittance is negligible due to the thickness of the Al, absorptance (A) can simply be estimated using reflectance alone as 1-R. Figure 2(a) shows the measured absorption spectra of the samples. The peak absorption frequency is found to be proportional to the inverse of the square size (1/s) as shown in Fig. 2(b). As the absorption is due to localized electromagnetic resonances, it is not surprising that the lowest order resonance frequency is related to the inverse of the square size. The exact explanation behind this absorption mechanism is still under debate and various models have been proposed such as impedance matching to free space[19], an equivalent RLC circuit[20], confined TM cavity modes[21], interference of multiple reflections[22], and transmission lines[23]. The lower frequency absorbers in this study reach nearly 100% absorption, but samples D and E (11 and 9 μm squares) reach 94% and 85% absorption, respectively. This is not entirely surprising, as the metamaterial parameters were optimized for configuration A. However, all of these models, as well as our numerical models, suggest it is possible to improve the absorption in Fig. 2 to 100% by slightly altering the thickness of the dielectric spacer and the periodicity of the metamaterial squares[12].

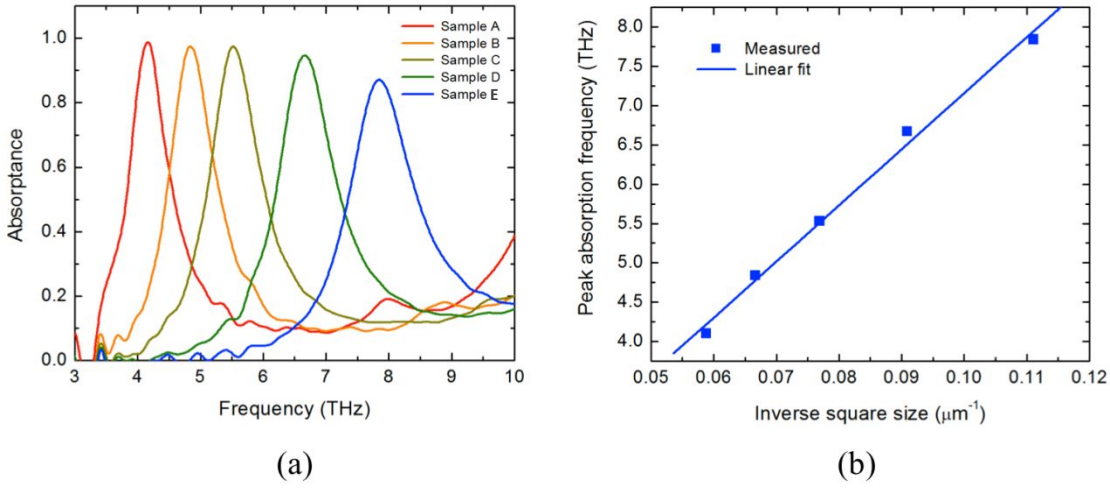

Figure 2. Absorption measurements (a) of configurations A-E (17-9μm squares) with an SiO_2 thickness of 1.6 μm and the linear relationship (b) between inverse square size and resonant frequency[18].

3.2 Emission measurements

The same Nexus 8700 FTIR was used to measure the emission characteristics of the metamaterial layers, albeit using a slightly different configuration. A gold-plated 90^0 f/1 off axis parabolic mirror with a focal length of 50 mm was used to collimate the sample emissions and direct them to the external port of the FTIR. A hot plate covered with front-side coated Al mirrors was used to heat the samples. The Al-coated mirrors have a low emissivity (~0.02) and thus shielded the FTIR from unwanted emissions from uncovered sections of the hot plate. For a reference emitter, a silicon wafer coated with black carbon was used to approximate a blackbody (BB). Emissivity spectra were calculated by dividing the sample emission by the black carbon emission at the same temperature. Figure 3 shows the emission measurements of samples A-E when heated to 400 ^{0}C, as well as the blackbody (BB) curve. Emittance is given in arbitrary units (a. u.) as the measurements are performed using standard Fourier transform spectroscopy where the detector is not calibrated.

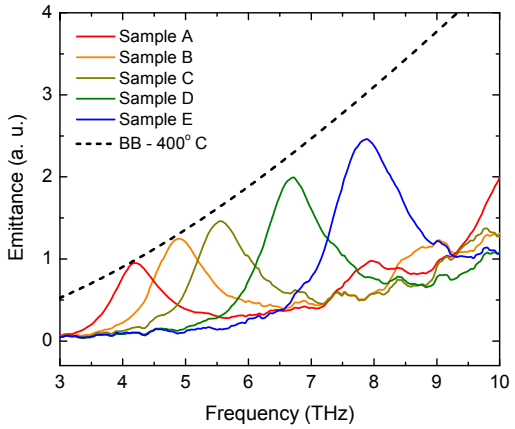

Figure 3. Emission measurements of samples A-E (17, 15, 13, 11, 9 μm squares, respectively) at 400 ºC. Blackbody curve at 400 ºC provided for reference.

4. DISCUSSION

4.1 Single band emitters

Kirchoff's law suggests that the narrowband absorption of Fig. 2(a) should be complimented by narrowband thermal emission[13]. Indeed, it is clear from Fig. 3 that the emitters do obey this law. Samples A-C approach, but not exceed the BB curve while samples D and E are emit significantly more THz, but has slightly lower emissivity as the other samples. To calculate the total power emitted in each THz band per unit area (P), Plank's blackbody radiation formula can be integrated with the frequency dependent emissivity ($\varepsilon(\nu)$):

$$P(\nu,T) = \frac{2\pi h}{c^2}\int \varepsilon(\nu)\nu^3 d\nu \Big/ \exp\left[h\nu/kT\right]-1. \quad (1)$$

where h is Plank's constant, k is Boltzmann's constant, and c is the speed of light in a vacuum. Using Eq. 1 for samples A, C, and E, the estimated emitted THz power per unit area at 400 ^{0}C is 11, 18 and 36 W/m^2, respectively. Therefore, a 4-inch wafer coated with these materials could produce an estimated 86, 145, and 280 mW of power, respectively, at 400 ^{0}C. In comparison, high power QCLs in the THz band produce about 5-10 mW average power[8,9], albeit from a much smaller area.

While it is apparent that Kirchhoff's law holds for these metamaterial layers, the temperature dependence of the emission is also important. Figure 4 shows sample A heated to 140, 280, and 400 ^{0}C. The peak emission frequency does not deviate appreciably from 4.2 THz, demonstrating that thermal expansion of the squares is negligible over these temperatures. In the Raleigh-Jeans[24] limit ($h\nu < kT$), Plank's law can be approximated by:

$$P(\nu,T) \approx \frac{2\pi kT\nu^2}{c^2}. \quad (2)$$

This results in a clear linear relationship between temperature and emitted power. Figure 4 does appear to show this linear relationship. As the photon energy of THz is very small to begin with (4-40 meV), this limit will almost

always apply allowing for easy calculation of emitted THz power. The quadratic dependence on the frequency of radiation, however, will severely limit the potential output at lower frequencies of THz.

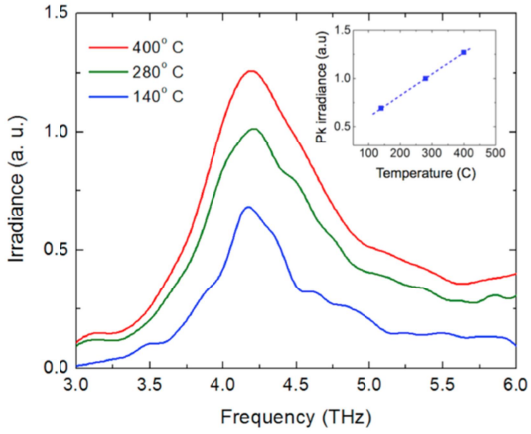

Figure 4. Spectral irradiance of Sample A, measured at 140, 280 and 400 °C. The inset shows that the measured peak emission (solid squares) depends linearly with temperature (solid line)[14].

Metamaterials can be very useful for tailoring the emission profile of a surface. Kirchhoff's law combined with the predictive power of FE simulations allows one to design metamaterials that emit the desired frequency of THz with bandwidth on the order of 1 THz. The plots in Fig. 5 compare how close emission measurements, absorption measurements, and FE simulations of absorption are to one another. This allows one to simply simulate the desired emission profile with great confidence before even fabricating the structure, as long as the material properties of the constituent materials are known. Of course, in practice, PECVD processes from different machines may yield slightly different optical properties. Therefore, care should be exercised when using these simulations to guide fabrication, despite their great predictive power.

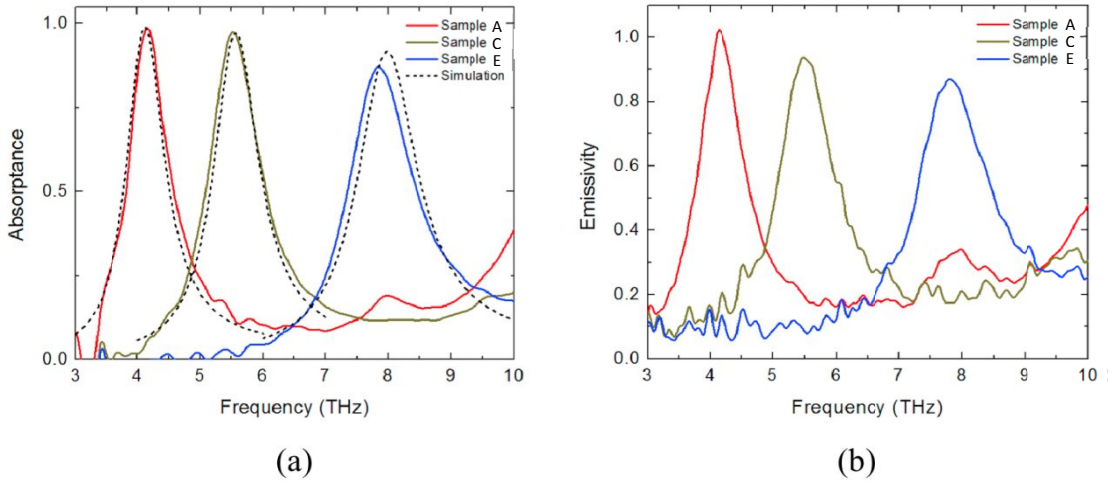

Figure 5. Spectral absorptance (a) and emissivity (b) of the metamaterial samples A, C and E. Solid lines represent the measured absorptance or emittance with peaks at 4.1, 5.4 and 7.8 THz respectively. Dashed lines represent the finite element simulation results. Adapted and reprinted from [14]

4.2 Complex emitter geometries

Although a single peak may be desired for many applications, multiple absorption peaks or an extended absorption peak may also be useful. To accomplish this, samples F and G make use of more than one square size in their geometry. As Fig. 6(a) shows, sample F has two clear emission peaks due to the two different square sizes in the geometry, 10 and 18 μm. Measured absorption in Fig. 6(b) for sample G, however, has 11, 14, and 17 μm squares in its configuration resulting in 3 distinct peaks. The dielectric spacer remains at the thickness of 1.6 μm for these emitters. It is clear that the peaks do not all share the same emissivity. This is due to the differing concentrations of each square on the surface in addition to coupling effects between squares of different sizes. Regardless, high emissivity is achieved for both samples at 400 ^{0}C, indicating that the reasoning applied to single band metamaterial emitters also applies in this case. Using FE simulations, one could thus create a metamaterial configuration to design and fabricate a surface with a custom THz emission signature.

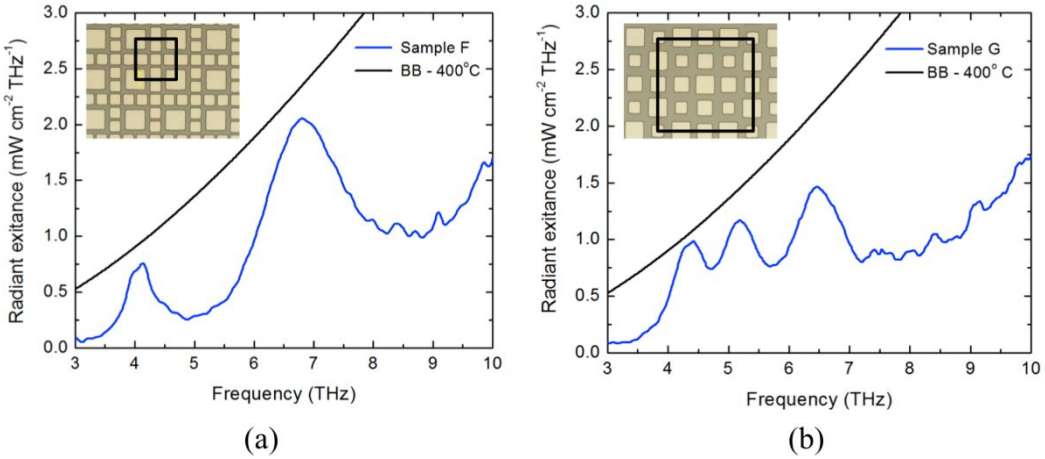

Figure 6. Radiant exitance of (a) dual band (sample G) and (b) triple metamaterials (sample F) at 400 ^{o}C. The dashed lines represent the blackbody curve at the same temperature. The insets show the micrographs of the two metamaterial structures used in the measurement.[18]

5. CONCLUSION

We have shown that metamaterial layers can serve as selective THz emitters following Kirchhoff's law. The FE simulations, absorptivity measurements, and emissivity measurements all agree, as expected. The emitted power of the metamaterials depends linearly on the temperature, as expected from the approximation of Plank's law at the Rayleigh-Jeans limit. The spectral characteristics do not change significantly, indicating that the thermal expansion of the metamaterials has a negligible impact in this range. FE simulations can thus be used to design metamaterials with the desired emission profile, not necessarily limited to a single band. These metamaterial layers can then be constructed using standard, well understood MEMS fabrication processes. Metamaterial emitters are therefore an attractive option for those that seek inexpensive narrowband or specifically tailored THz sources.

ACKNOWLEDGMENTS

This work is supported in part by a grant from the NRO. The authors would like to thank Brett Borden and James Luscombe for helpful discussions and Nick Lavrik and Sam Barone for technical assistance. A portion of this research was conducted at the Center for Nanophase Materials Sciences, which is sponsored at Oak Ridge National Laboratory by the Scientific User Facilities Division, Office of Basic Energy Sciences, U.S. Department of Energy.

REFERENCES

[1] Federici, J.F., Schulkin, B., Huang, F., Gary, D., Barat, R., Oliveira, F. and Zimdars, D., "THz imaging and sensing for security applications--explosives, weapons, and drugs," Semicond. Sci. Technol. 20, S266-S280(2005)

[2] Kim, S. M., Hatami, F., Harris, J. S., Kurian, A. W., Ford, J., King, D., Scalari, G., Giovannini, M., Hoyler, N., Faist, J., and Harris, G., "Biomedical terahertz imaging with a quantum cascade laser," Appl. Phys. Lett. 88, 153903(2006)

[3] Taylor, Z. D., Singh, R. S., Culjat, M. O., Suen, J. Y., Grundfest, W. S., Lee, H. and Brown, E. R., "Reflective terahertz imaging of porcine skin burns," Opt. Lett. 33(11), 1258-1260(2008)

[4] Bjarnason, J. E., Chan, T. L. J., Lee, A. W. M., Celis, M. A. and Brown, E. R., "Millimeter-wave, terahertz, and midinfrared transmission through common clothing," Appl. Phys. Lett. 85, 519 (2004).

[5] Clothier, R. H. and Bourne, N., "Effects of THz exposure on human primary keratinocyte differentiation and viability," J. Biol. Phys. 29, 179–85 (2003).

[6] Davies, A. G. and Linfield, E. H., "Bridging the terahertz gap," Phys. World **14**, 37-41 (2004).

[7] Shur, M. S. and Ryzhii, V., " New concepts for submillimeter-wave detection and generation," in Proceedings of 11th GaAs applications symposium, Munich (2003), 301-304.

[8] Williams, B. S., "Terahertz quantum-cascade lasers," Nature Photon. **1**(9), 517-525 (2007).

[9] Kumar, S., "Recent progress in terahertz quantum cascade lasers," IEEE J. Sel. Topics Quantum Electron. **17**(1), 38-47 (2011).

[10] Kohler, R., Tredicucci, A., Beltran, F., Beere, H. E., Linfield, E. H., Davies, A. G., Ritchie, D. A., Iotti, R. C. and Rossi, F., "Terahertz semiconductor-heterostructure laser," Nature **417**, 156-159 (2002).

[11] Carr, G. L., Martin, M. C., McKinney, W. R., Jordan, K., Neil, G. R. and Willians, G. P., "High-power terahertz radiation from relativistic electrons," Nature **420**, 153-156 (2002).

[12] Kearney, B., Alves, F., Grbovic, D. and Karunasiri, G., "Al/SiOx/Al Single and Multiband Metamaterial Absorbers for THz Sensor Applications," Opt. Eng. In Press.

[13] Kirchhoff, G., "On the relation between the radiating and the absorbing powers of different bodies for light and heat," Philos. Mag. **20**, 1–21 (1860).

[14] Alves, F., Kearney, B., Grbovic, D., and Karunasiri, G., "Narrowband terahertz emitters using metamaterial films," Opt. Expr. **20**(19), 21025-21032 (2012).

[15] Gunde, M. K. and Macek, M., "Infrared optical constants and dielectric response functions of silicon nitride and oxynitride films," Phys. Status Solidi A **183**, 439–449 (2001).

[16] Smith, D. Y., Shiles, E., and Inokuti, M., "Silicon Dioxide (SiO2)," in [Handbook of Optical Constants of Solids Part 2], E. D. Palik, ed., Academic (1998).

[17] Kitamura, R., Pilon, L. and Jonasz, M., "Optical constants of silica glass from extreme ultraviolet to far infrared at near room temperature," Appl. Opt. **46**(33), 8118–8133 (2007).

[18] Karunasiri, G., Alves, F., Kearney, B., and Grbovic, D., "A Review on Narrowband Terahertz Emitters," to be published.

[19] Landy, N.I., Sajuyigbe, S., Mock, J.J., Smith, D. R. and Padilla, W.J., "Perfect Metamaterial Absorber," Phys. Rev. Lett. 100, 207402(2008)

[20] Alves, F., Kearney, B., Grbovic, D., Lavrik, N. V. and Karunasiri, G., "Strong terahertz absorption using thin metamaterial structures," Appl. Phys. Lett. 100, 111104(2011).

[21] Todorov, Y., Tosetto, L., Teissier, J., Andrews, A. M., Klang, P., Colombelli, R., Sagnes, I., Strasser, G., and Sirtori, C., "Optical porperties of metal-dielectric-metal microcavities in the THz frequency range," Opt. Expr. 18(13), 13886(2010)

[22] Chen, H.-T., "Interference theory of metamaterial perfect absorbers," Opt. Expr. 20(3), 7165-7172 (2012)

[23] Wen, Q.-Y, Xie, Y.-S, Zhang, H.-W., Yang, Q.-H, Li, Y.-X., Liu, Y.-L., "Transmission line model and fields analysis of metamaterial absorber in the terahertz band," Opt. Expr. 17(22), 20256-20265 (2009)

[24] Palmer, J. M. and Grant, B. G., [The Art of Radiometry], ed. ,SPIE Press (2010).